Electronic Supplementary Information for

Smart crystalline framework materials with triazole carboxylic acid ligand: fluorescence sensing and catalytic reduction of PNP

Qiu Lv[#1], Qing Lin Guan[#1], Jin Long Li, Jin Xiao Li, Jing Jin*, Feng Ying Bai*, Yong Heng Xing

Qiu Lv[#1] and Qing Lin Guan[#1] contributed equally to this work.

College of Chemistry and Chemical Engineering, Liaoning Normal University, Dalian, 116029, P. R. China

Supplementary Index

Materials and Measurements

All starting materials were of reagent grade quality and were obtained from commercial sources without further purification. P-nitrophenol (PNP) and metal salts ($Pb(NO_3)_2$, $Co(NO_3)_2 \cdot 6H_2O$, $Cu(NO_3)_2 \cdot 3H_2O$) are chemically toxic reagents, standard precautions for handling the materials must be strictly followed, and all experiments were carried out in a fume hood. The powder X-ray diffraction patterns (PXRD) of 1-3 were obtained on Advance-D8 equipped with Cu-Kα radiation, and the range was 5° <2θ <50°, with a step size of 0.02° (2θ) and a count time of 2 s per step at room temperature. All IR measurements were obtained using a Bruker AXS TENSOR-27 FT-IR spectrometer with pressed KBr pellets in the range of 400-4000 cm-1 at room temperature. UV-vis-NIR spectra were recorded on a JASCOV-570 UV/vis/NIR microspectrophotometer (200-2500 nm). Liquid UV-visible absorption spectroscopy was performed on SPECORD 250/PLUS. The maximum absorption wavelength of the PNP solution was measured on spectrophotometer UV-1000. Thermogravimetric analysis (TG) was performed on a PerkinElmer Diamond TG/DTA under N_2 atmosphere from 30 °C to 800 °C with a heating rate of 10 °C/min. Fluorescence spectra were measured on a JASCO FP-4600 and HORIBA Fluoromax-4-TCSPC fluorimeter.

Preparation of Ligand H_2MCTCA

The specific synthesis method includes two steps: synthesis of azide benzoic acid by intermediate and ring reaction of triazolium. The specific synthesis route of H_2MCTCA as shown in Scheme S1.

Preparation of p-azide benzoic acid: Firstly, a mixture of PABA (6.86g, 0.05mol) and 19 mL 12 mol/L HCl was add to a 100 mL three-neck flask, and then was stirred in ice water bath (0-5 ℃) until all solids are dissolved. Then $NaNO_3$ (3.45g, 0.04mol) was dissolved in 10 mL of deionized water and transferred to a constant pressure dropping funnel, and then slowly added to a three-mouth flask. After drip adding, stir in ice water for 30 min and then filter. Transfer filtrate to three-necked flask keeping ice water cool. NaN_3 (3.25g, 0.05mol) was dissolved in 10 mL of deionized water, dropping it into the filtrate and continue to stir for 2 h. After the reaction was complete, the insoluble matter was removed by suction filtration, and dried to obtain 6.40 g of white solids with a yield of 78.10%.

Triazole ring reaction: The metallic Na (30 g) was added to 10 mL anhydrous ethanol until no gas was produced to obtain sodium ethanol solution, which was transferred to a three-necked flask and mixed with ethyl acetoacetate (1.31 g, 0.01 mol). The p-azide benzoic acid (1.63 g, 0.01 mol) prepared in step 1 was added to the mixed solution under an ice water bath, stirring for 30 min. Then three-necked was transferred to the oil bath and refluxed at 100 °C for 2 h. After the reaction,filtrate was obtain by suction filtration, and then the pH of filtrate was adjusted to 5-6 with 12 mol/L concentrated hydrochloric acid, light yellow solid was obtained after vacuum filtration. By recrystalization in ethanol and drying, obtained the target product 2.30 g H_2MCTCA with a yield of 93%. The ^{1}H-NMR, ^{13}C-NMR and solid-state fluorescence spectra of the ligand H_2MCTCA are shown in Figure S1-S3.

According to the ^{1}H-NMR hydrogen spectrum, four different chemical environments of H were found in this compound. Among them, 2.55 ppm is the aliphatic proton peak, which is presumed to be $-CH_3$, so the area of this peak is taken as unit 3 for integral analysis. There were two sharp bimodal peaks at 8.17 ppm and 7.78 ppm, and the integrated areas were 2.37 and 2.38, respectively. The coupling field numbers were all 8.6Hz, which was speculated to be four protons on the benzene ring. There is a wide peak at 13.25 ppm with an integral area of 2.32, which is presumed to be caused by the superposition of two free -OH. ^{1}H NMR (400 MHz, DMSO-d_6) δ 13.25 (s, 2H), 8.17 (d, J = 8.6 Hz, 2H), 7.78 (d, J = 8.6 Hz, 2H), 2.55 (s, 3H).

According to the ^{13}C-NMR spectrum, nine carbon atoms in different chemical environments were found in this compound. Among them, 9.77 ppm is fatty carbon, namely $-CH_3$, which is taken as unit 1 for carbon spectrum analysis. At 131.98, 130.64, 130.57, 130.40 and 125.40 ppm, the carbon atoms of benzene ring connected with them were shifted to 139.14 ppm due to the influence of triazolium heterocyclic ring. At 138.56 and 136.79 ppm, there are two carbon atoms on the heterocyclic ring of triazole. There are two carboxyl carbon atoms at 166.32 and 162.46 ppm. ^{13}C-NMR (101 MHz, DMSO-d_6) δ 166.32, 162.46, 139.14, 138.56, 136.79, 131.98, 130.64, 130.57, 130.40, 125.40, 9.77.

Then, the excitation and emission spectra of the ligand H_2MCTCA were monitored at room temperature. In Figure. S3, when the excitation wavelength is 280 nm, ligand H_2MCTCA shows the strongest emission peak at 385 nm.

X-ray Crystallographic Determination

All single-crystal X-ray diffraction data were collected at room temperature on a Bruker AXS SMART APEX II CCD diffractometer with graphite monochromatized Mo-Kα radiation (λ=0.71073Å). Data collection and cell parameter determinations were performed using the SMART program[1]. The diffraction intensity data was corrected by Lp factor, and the crystal structure was solved by direct method and difference Fourier synthesis method. All the non-hydrogen coordinates and anisotropic temperature factors were corrected by the full matrix and least square method. All the non-hydrogen coordinates were determined by theoretical hydrogenation program. All calculations were performed on the OLEX2 platform using SHELX-97 program[2]. We used RIGU and FLAT instructions to limit the C, N and O of the ligand, and we used DANG and DFIX instructions to limit the length of the C-C, O-O and C-O bond. OMIT instructions are also added to the complex to remove undesirable reflection affected by beam stopping. The PLATON was used to check the structure for additional symmetry[3]. The hydrogen bonds and other weak interactions between molecules, the coordination patterns of ligands and the structure diagrams of complexes were drawn using Diamond 3.2 program. The main parameters of crystal structure refinement are:

$$S=[\sum W(Fo^2-Fc^2)^2/(n-p)]^{1/2} \quad (1\text{-}1)$$
$$R_1=\sum|\,|Fo|-|Fc|\,|/\sum|Fo| \quad (1\text{-}2)$$
$$wR_2=[\sum w(Fo^2-Fc^2)^2/\sum w(Fo^2)^2]^{1/2};\ [Fo > 4\sigma(Fo)] \quad (1\text{-}3)$$
$$Rw=[\sum(|Fo|-|Fc|)^2/\sum|Fo|^2]^{1/2} \quad (1\text{-}4)$$
$$P=[max\ (Fo^2, 0) + 2\ (Fc^2)]/3 \quad (1\text{-}5)$$

n: the number of reflections

In addition, during testing crystal, the crystals could weather, resulting in poor data quality. Due to the extremely difficult cultivation of this crystal, crystal data collections have found that the diffraction points are relatively weak and there are no points at high angles, which resulting in the attached Fobs vs Fcalc not a narrow straight line (Figure S19). Therefore, the crystallographic parameters have not achieved good results, despite our efforts to refine it. The main crystallographic data and related bond length data of the complexes **1-3** are shown in the Table S1-S3. CCDC 2280257, 2280241 and 2280242 contained crystallographic data for this work.

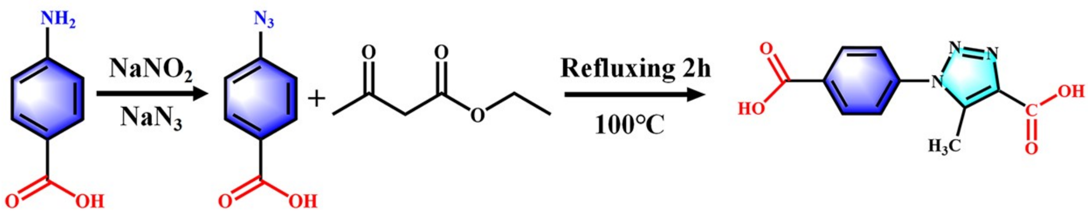

Scheme S1. Synthetic routes of H_2MCTCA ligand.

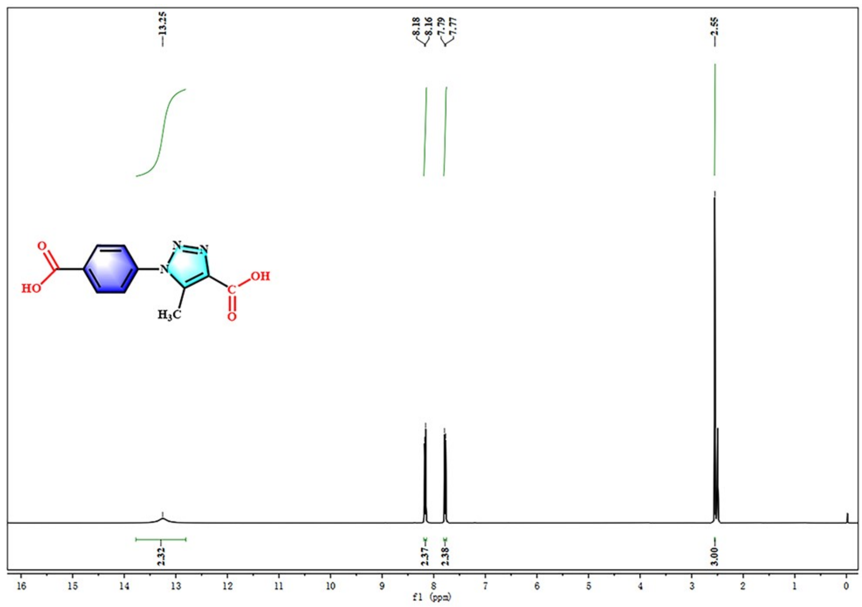

Figure S1. The ^{1}H-NMR spectrum of H_2MCTCA ligand.

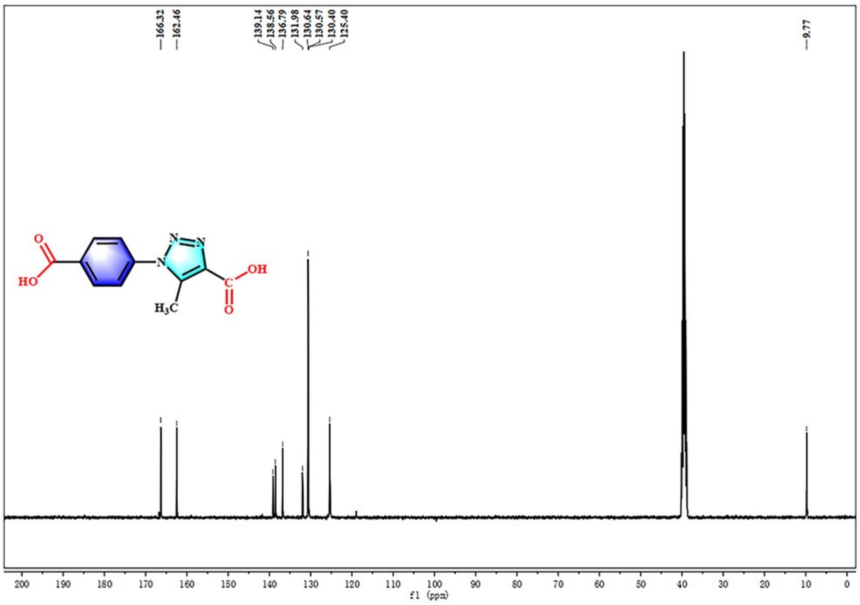

Figure S2. The ^{13}C-NMR spectrum of H_2MCTCA ligand.

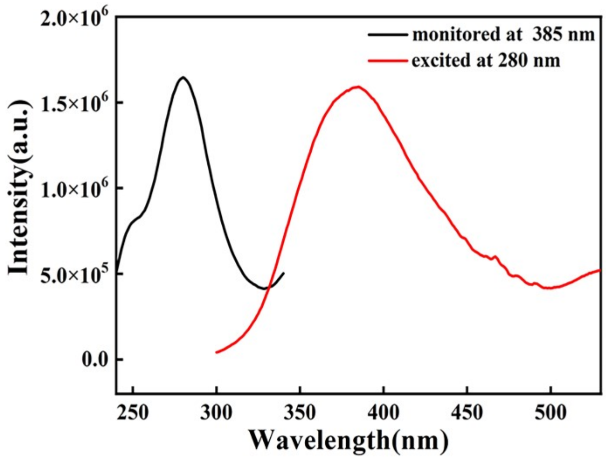

Figure S3. The solid-state fluorescence spectrum of H_2MCTCA.

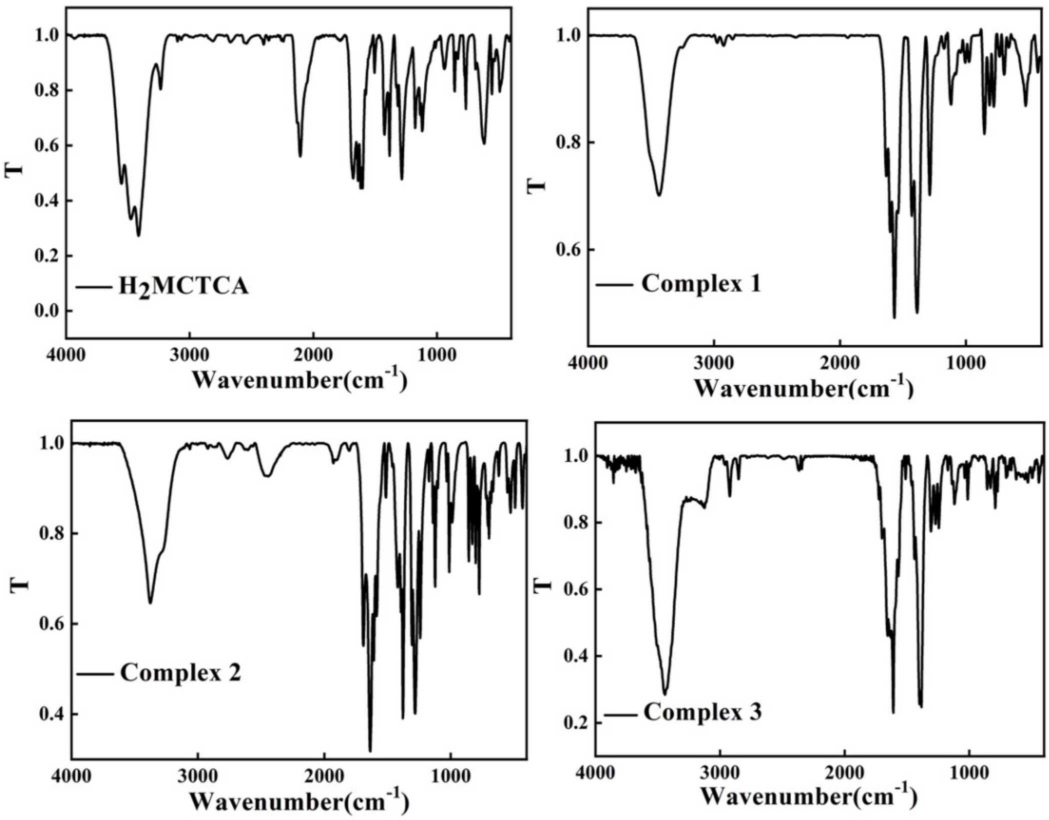

Figure S4. The IR spectra of H_2MCTCA and complexes **1-3**.

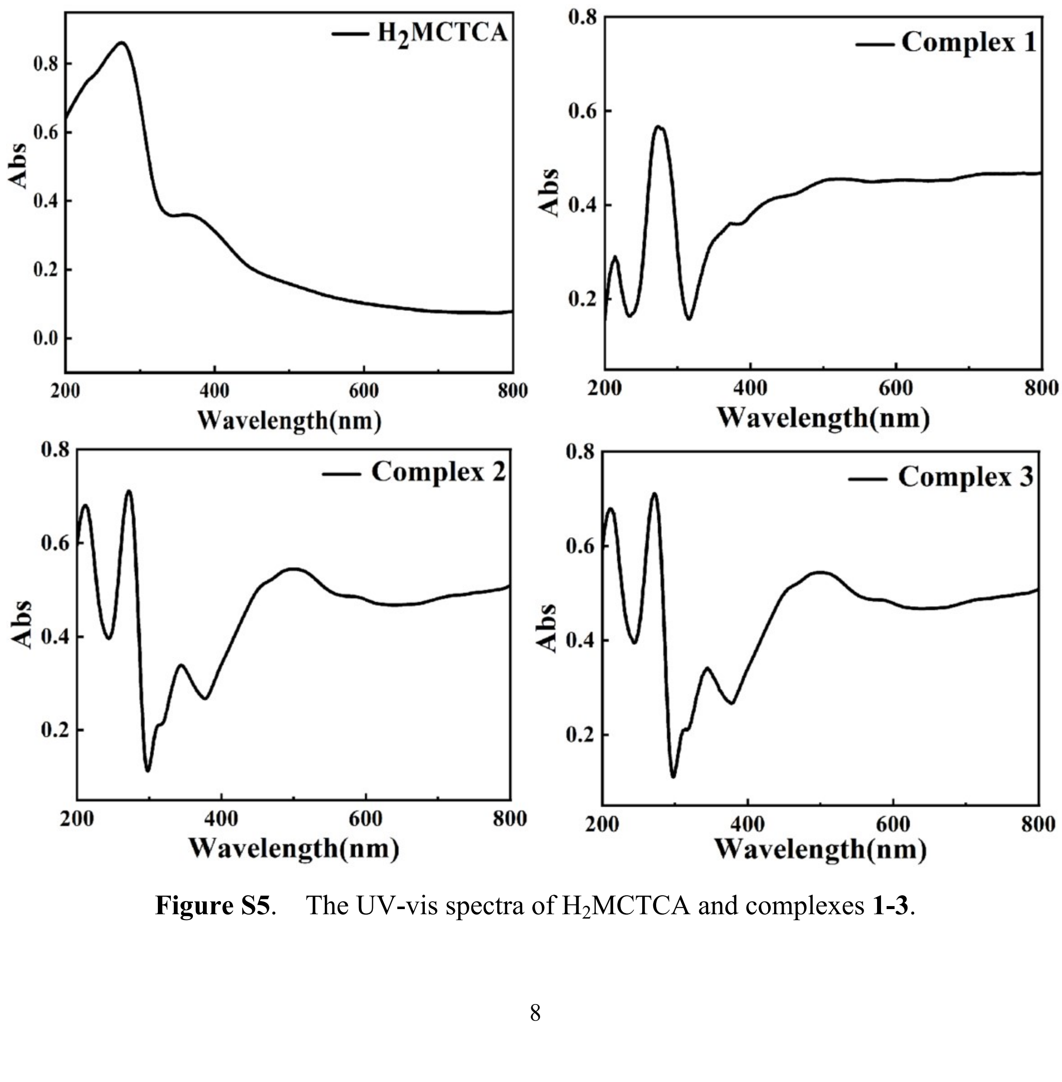

Figure S5. The UV-vis spectra of H_2MCTCA and complexes **1-3**.

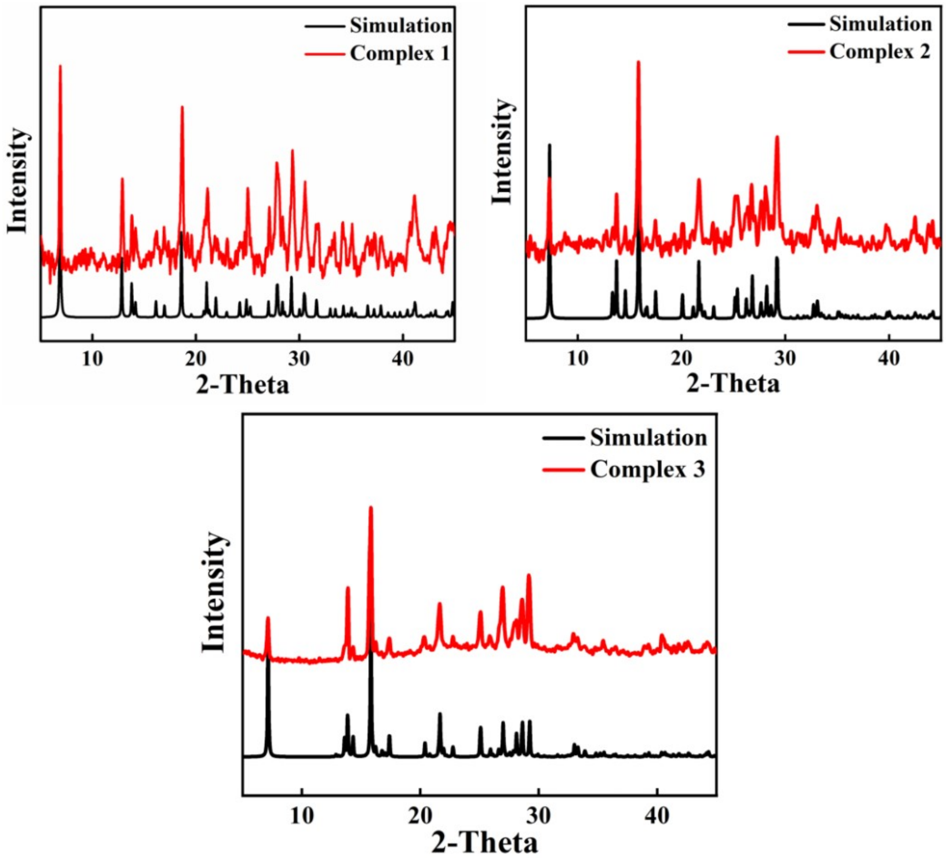

Figure S6. The PXRD patterns of complexes **1-3.**

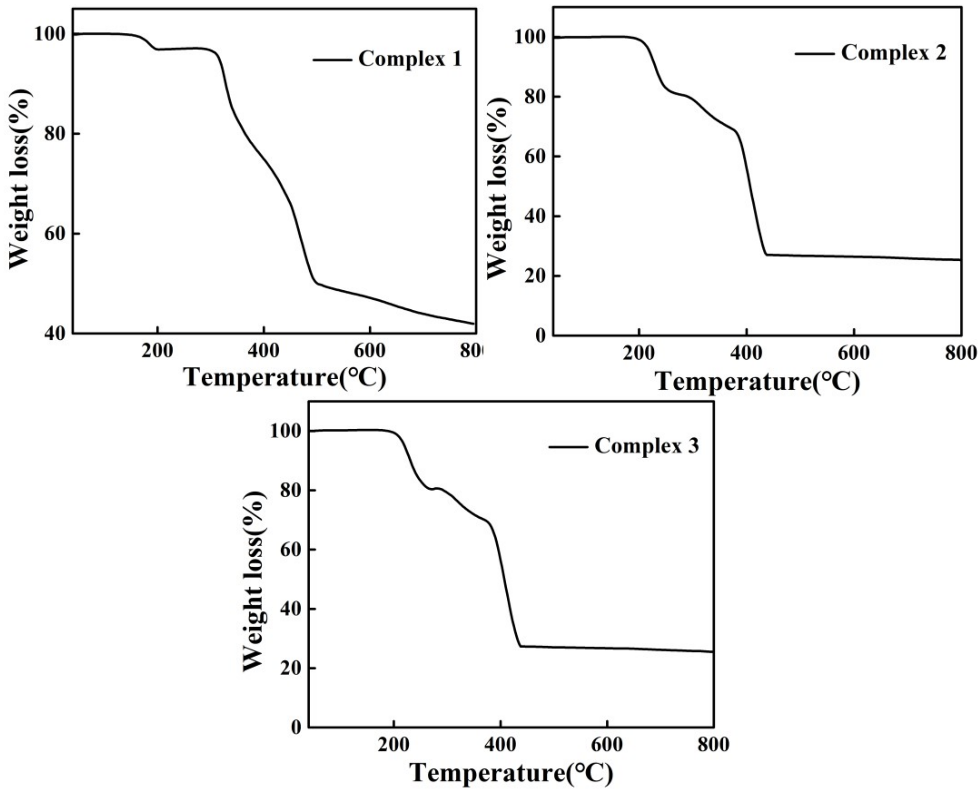

Figure S7. The TG curves of complexes **1-3**.

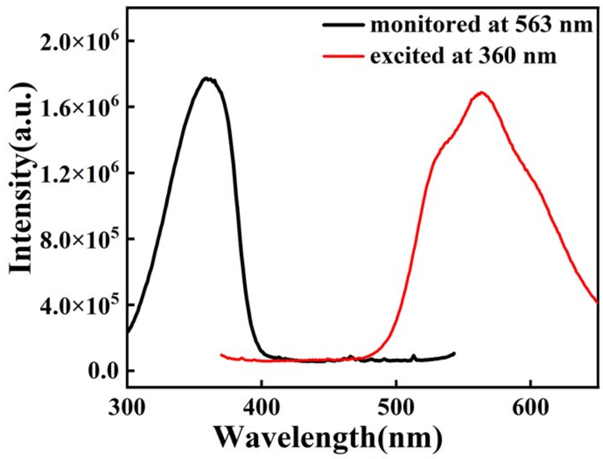

Figure S8. The solid-state fluorescence spectra of complex **1**.

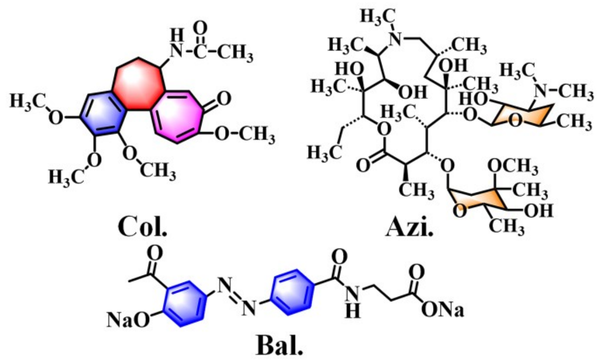

Figure 9. The structures of three small-molecule drugs.

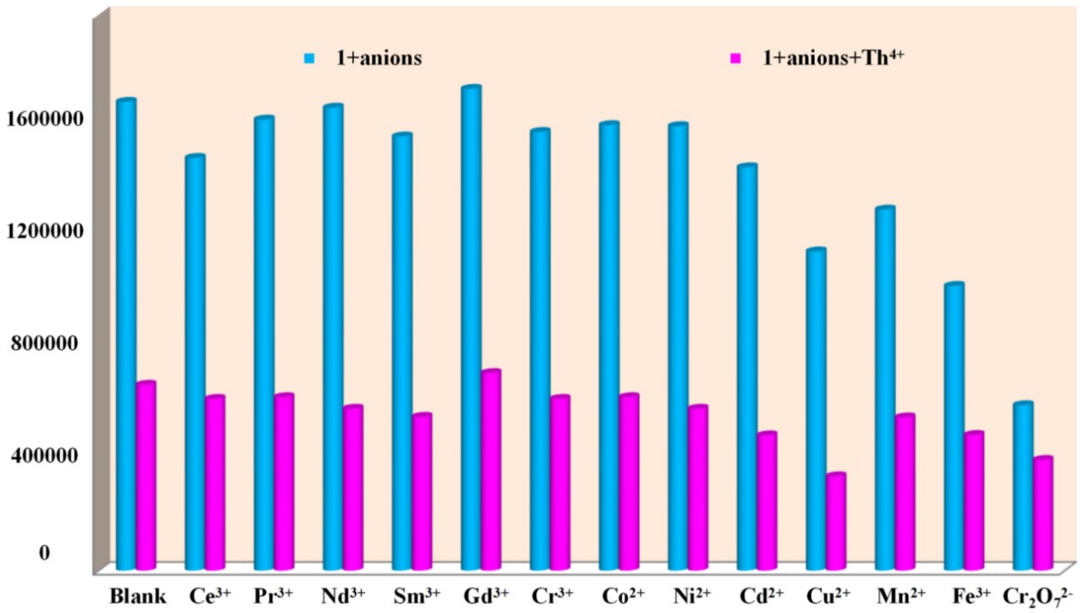

Figure S10. The fluorescence intensity at 563 nm after adding different metal ions and adding Th^{4+} in the presence of interfering ions.

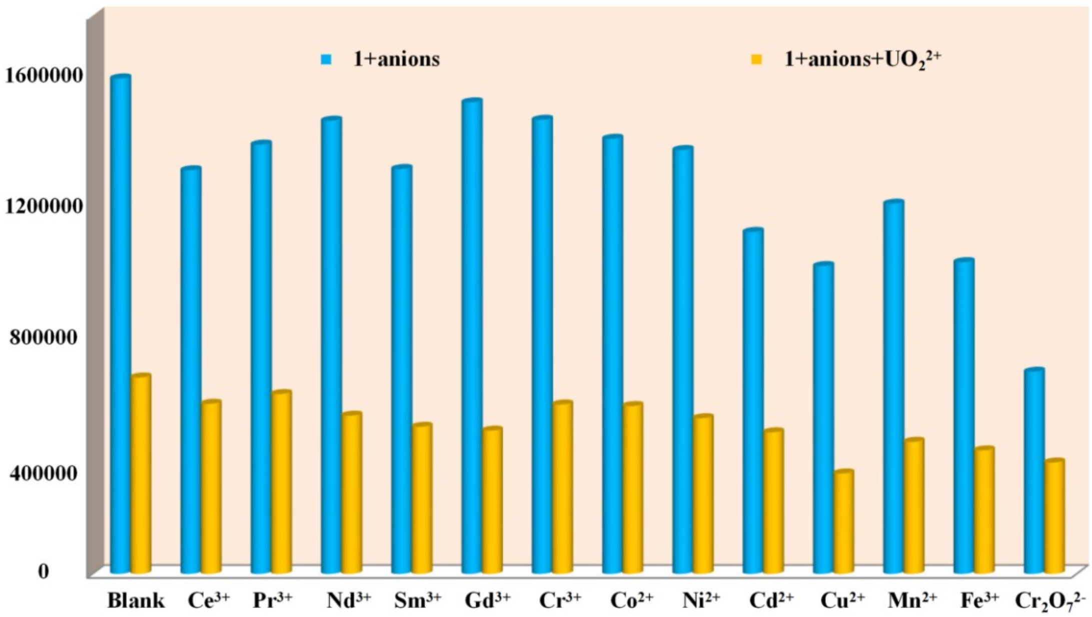

Figure S11. The fluorescence intensity at 563 nm after adding different metal ions and adding UO_2^{2+} in the presence of interfering ions.

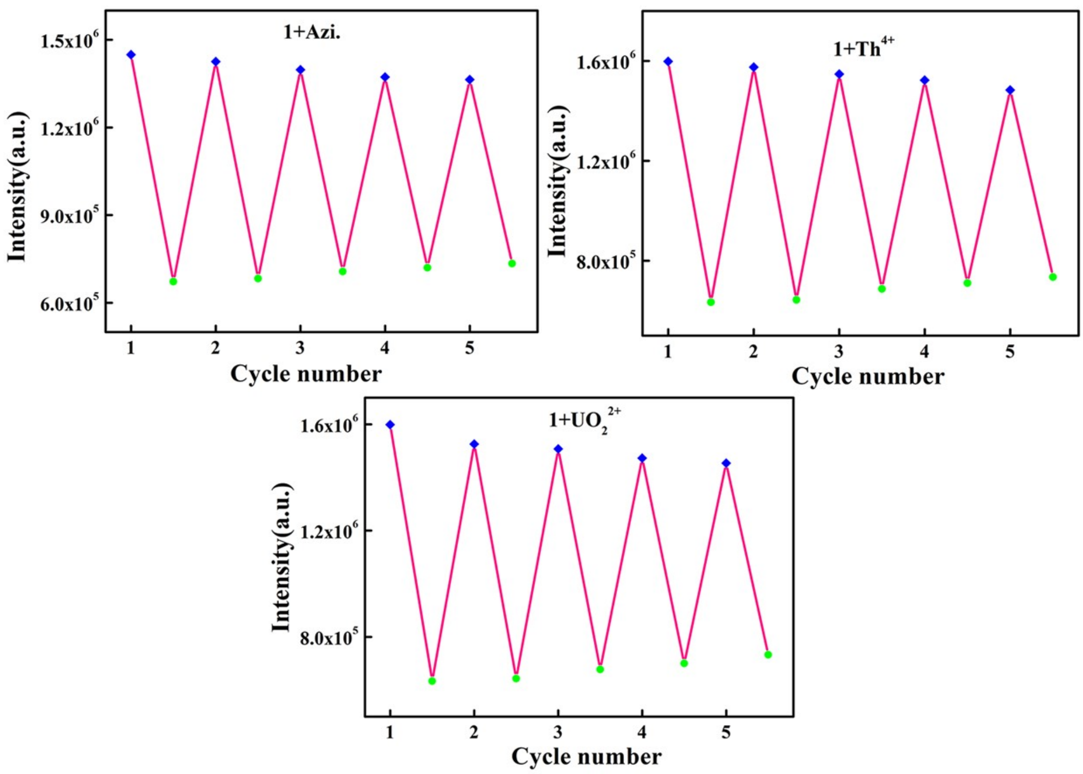

Figure S12. Reusability experiments of detecting Azi. ,Th^{4+} and UO_2^{2+}.

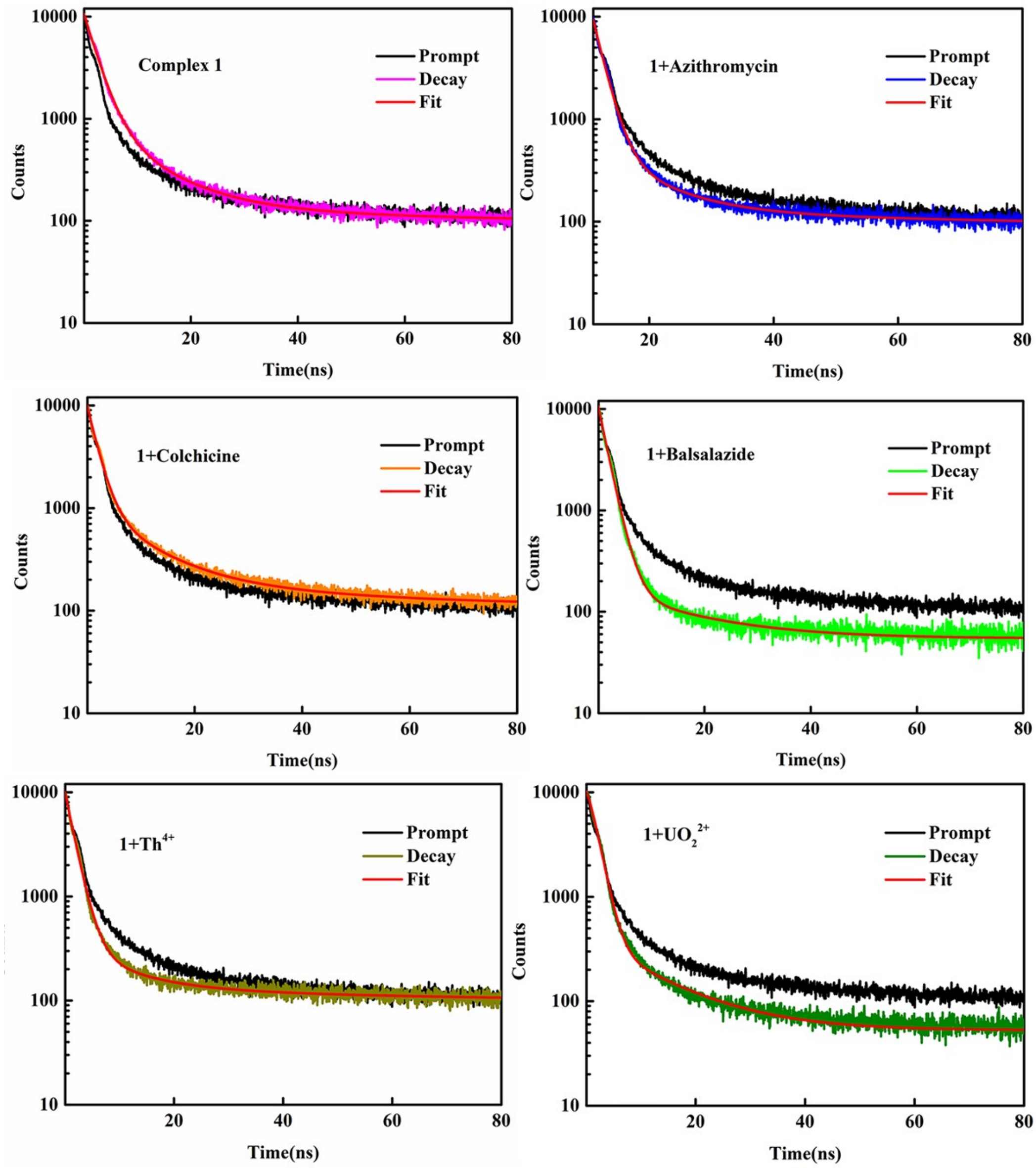

Figure S13. Lifetime decay curves of complex **1** before and after detection.

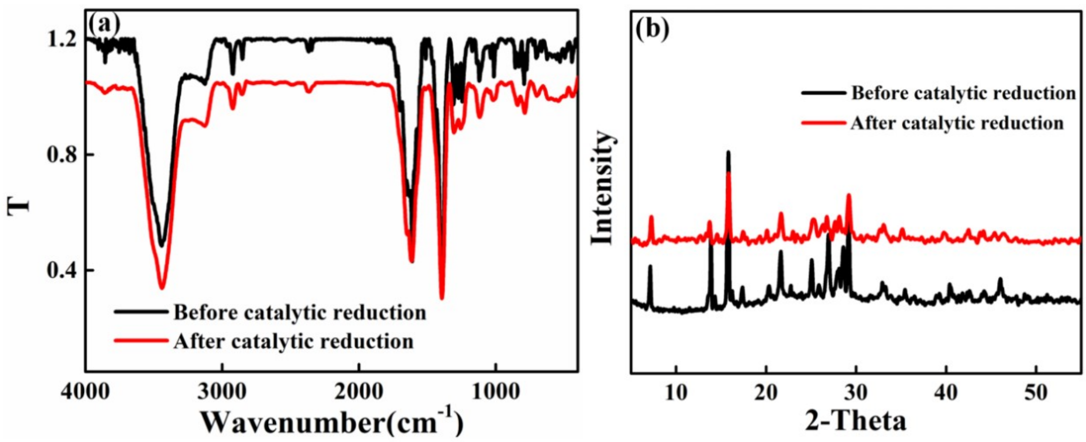

Figure S14. (a) IR spectra before and after catalytic reaction of complex **3**; (b) PXRD pattern before and after catalytic reaction of complex **3**.

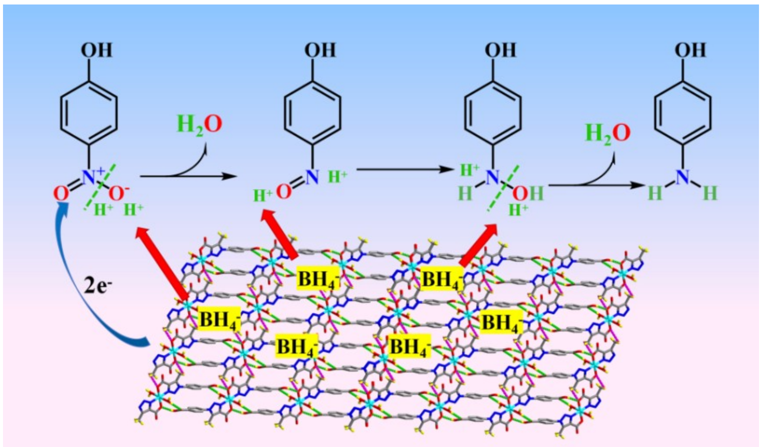

Figure S15. Details of electron gain and loss during PNP reduction.

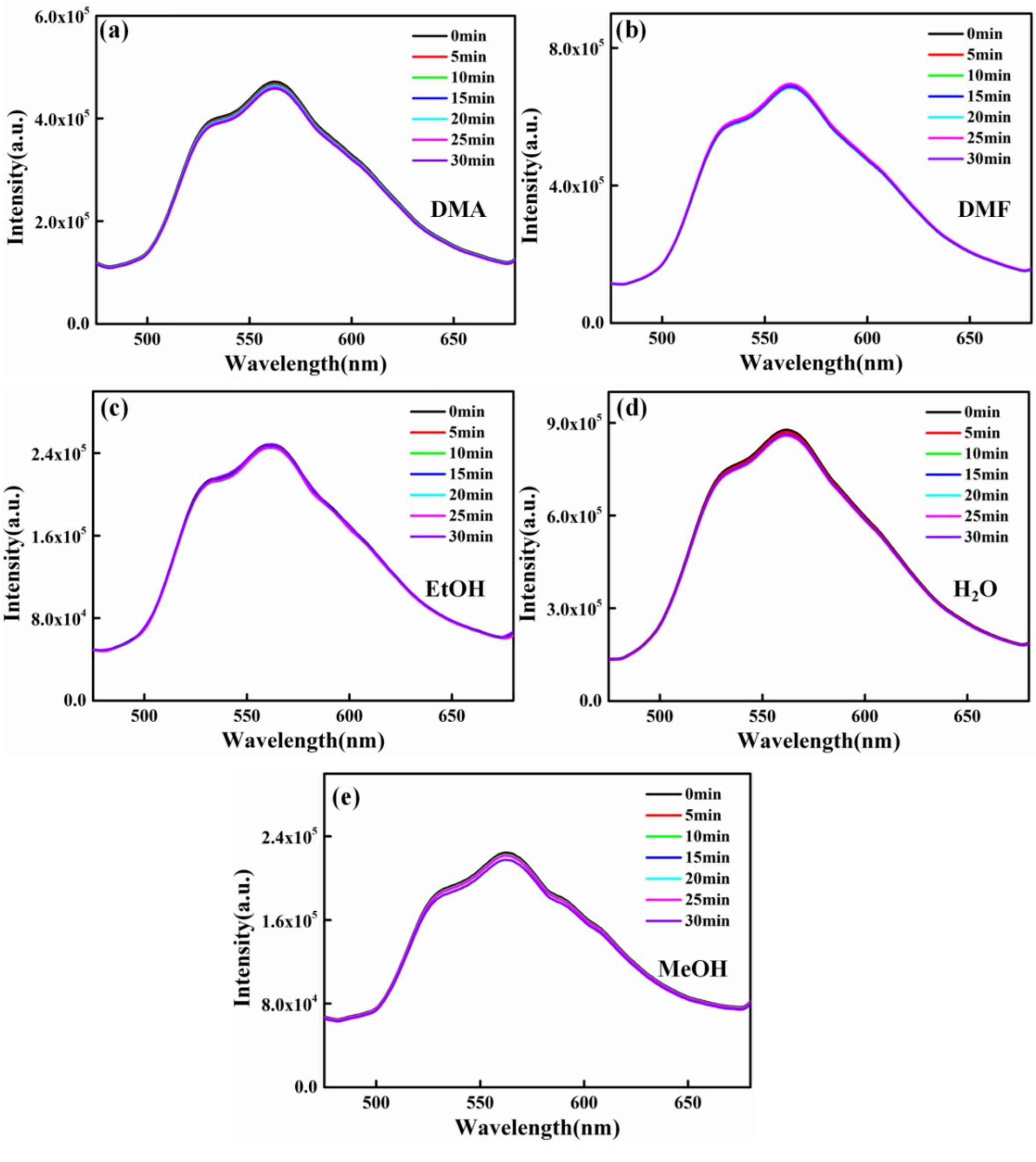

Figure S16. Fluorescence intensity of complex **1** suspension at 563 nm in different solvents for 30 min.

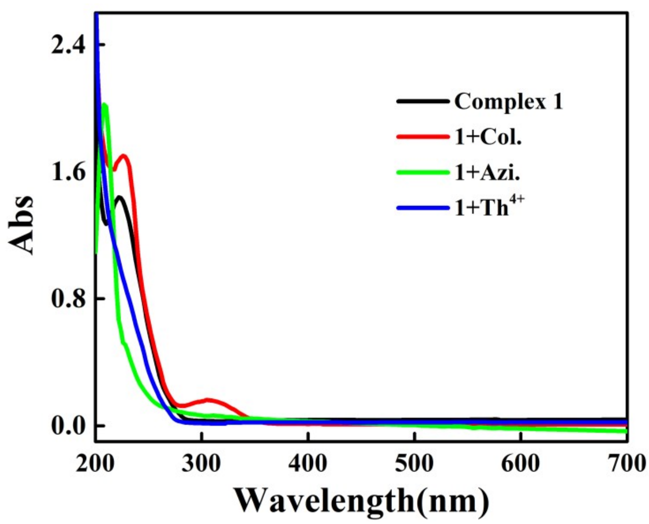

Figure S17. UV-vis absorption spectra of complex **1** after addition of analytes.

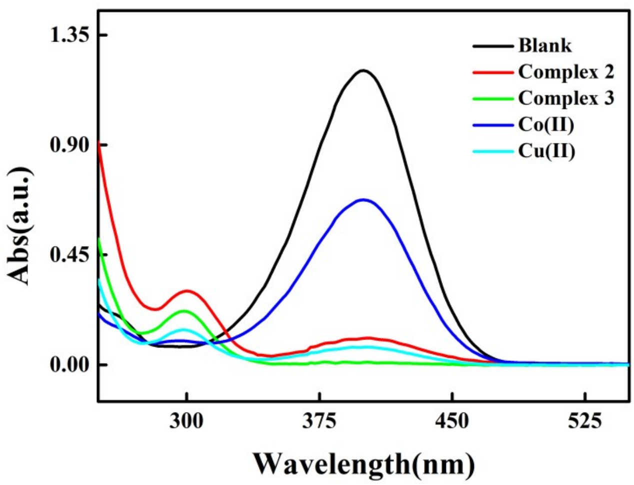

Figure S18. The UV-vis spectra of complexes and raw metal salts catalytic reduction of PNP in 10 min.

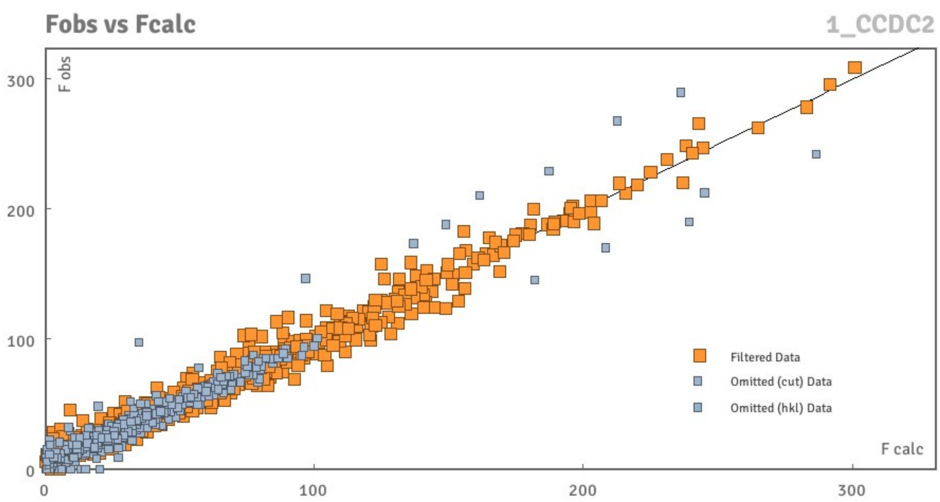

Figure S19. The attached Fobs vs Fcalc plot of complex **1**.

Table S1. Single crystal cell parameters for the complexes **1-3.**

Complexes	**1**	**2**	**3**
Formula	$C_{11}H_9N_3O_5Pb$	$C_{22}H_{20}CoN_6O_{10}$	$C_{22}H_{20}CuN_6O_{10}$
M (g mol^{-1})	470.40	587.37	591.98
Crystal system	*Orthorhombic*	*Triclinic*	*Triclinic*
Space group	*Pnma*	$P\bar{1}$	$P\bar{1}$
a (Å)	6.596(2)	6.9869(7)	6.8933(5)
b (Å)	7.151(2)	7.2719(8)	7.3208(5)
c (Å)	25.646(8)	12.7840(13)	13.1213(8)
α (°)	90	103.327(2)	104.634(10)
β (°)	90	98.837(2)	98.637(10)
γ (°)	90	103.314(2)	104.382(10)
Z	4	1	1
D_{calc}	2.583	1.625	1.626
F(000)	872.0	301.0	303.0
μ(Mo-Kα) /mm^{-1}	13.972	0.786	0.974
2θ (°)	5.914-52.742	5.99-62.4	5.93-62.006
Reflections collected	5562	4175	4190
$\Delta(\rho)$ (e Å^{-3})	1.69 and -2.37	0.41 and -0.26	0.44 and -0.46
Goodness of fit	1.095	1.080	1.055
R_1[a]	0.0686	0.0337	0.0354
wR_2[a]	0.1916	0.0951	0.0939

*[a] $R_1=\Sigma||Fo|-|Fc||/\Sigma|Fo|$, $wR_2=[\Sigma w(Fo^2-Fc^2)^2/\Sigma w(Fo^2)^2]^{1/2}$; $[Fo>4\sigma(Fo)]$. [b] Based on all data.

Table S2. Selected bond distances (Å) of complexes **1-3.**

Complex 1			
Pb-O1	2.455(5)	Pb-O3	2.515(5)
Pb-O2	2.686(5)	Pb-O4	2.623(5)
Pb-O3#1	2.702(4)	Pb-O5#2	2.625(5)
Complex 2			
Co-O3#1	2.0794(11)	Co-O3	2.0793(10)
Co-O5#1	2.1112(13)	Co-O5	2.1112(13)
Co-N3#1	2.1305(11)	Co-N3	2.1305(11)
Complex 3			
Cu-O4	1.9883(12)	Cu-O5	2.3817(18)
Cu-O4#1	1.9882(12)	Cu-O5#1	2.3817(18)
Cu-N3#1	2.0012(13)	Cu-N3#1	2.0012(13)

Symmetry transformations used to generate equivalent atoms for complex **1**: #1, -1-x, -1-y, 1-z; #2, 1+x, y, z; for complex **2**: #1, 2-x, 2-y, 2-z; for complex **3**: #1, -x, -y, -z.

Table S3. Selected bond angle (°) for complexes **1-3.**

Complex 1			
O1-Pb-O2	50.77(16)	O3-Pb-O4	80.73(15)
O1-Pb-O3$^{\#1}$	77.87(15)	O3-Pb-O4	149.00(15)
O1-Pb-O3	73.62(16)	O3-Pb-O5$^{\#2}$	107.55(16)
O1-Pb-O4	80.00(16)	O4-Pb-O2	149.84(15)
O1-Pb-O5$^{\#2}$	100.75(17)	O4-Pb-O3$^{\#1}$	68.28(16)
O2-Pb-O3$^{\#1}$	73.12(15)	O4-Pb-O5$^{\#2}$	72.90(16)
O3-Pb-O2	119.38(15)	O5$^{\#2}$-Pb-O2	136.12(14)
O3-Pb-O3$^{\#1}$	73.55(17)	O5$^{\#2}$-Pb-O3$^{\#1}$	
Complex 2			
O3-Co-O3$^{\#1}$	180.0(8)	N3-Co-O3$^{\#1}$	102.03(4)
O3-Co-O5$^{\#1}$	93.45(4)	N3$^{\#1}$-Co-O3	102.03(4)
O3$^{\#1}$-Co-O5	93.57(4)	N3$^{\#1}$-Co-O5	87.60(5)
O5-Co-O3	86.55(4)	N3-Co-O5$^{\#1}$	87.60(5)
O5$^{\#1}$-Co-O3$^{\#1}$	86.55(4)	N3$^{\#1}$-Co-O5$^{\#1}$	92.40(5)
O5-Co-O5$^{\#1}$	180.0	N3-Co-O5	92.40(5)
N3$^{\#1}$-Co-O3$^{\#1}$	77.97(4)	N3-Co-N3$^{\#1}$	180.0
N3-Co-O3	77.97(4)		
Complex 3			
O4-Cu-O4$^{\#1}$	180.00	N3-Cu-O4$^{\#1}$	98.36(5)
O4-Cu-O5$^{\#1}$	85.97(6)	N3$^{\#1}$-Cu-O4	98.36(5)
O4$^{\#1}$-Cu-O5	85.97(6)	N3$^{\#1}$-Cu-O5	86.95(6)
O5-Cu-O4	94.03(6)	N3-Cu-O5$^{\#1}$	86.95(6)
O5$^{\#1}$-Cu-O4$^{\#1}$	94.03(6)	N3$^{\#1}$-Cu-O5$^{\#1}$	93.05(6)
O5-Cu-O5$^{\#1}$	180.0	N3-Cu-O5	93.05(6)
N3$^{\#1}$-Cu-O4$^{\#1}$	81.64(5)	N3-Cu-N3$^{\#1}$	180.0
N3-Cu-O4	81.64(5)		

Symmetry transformations used to generate equivalent atoms for complex **1**: #1, -1-x, -1-y, 1-z; #2, 1+x, y, z; for complex **2**: #1, 2-x, 2-y, 2-z; for complex **3**: #1, -x, -y, -z.

Table S4. Detailed attribution of the IR (cm^{-1}) spectra of H_2MCTCA and complexes **1-3.**

Complexes	H_2MCTCA	**1**	**2**	**3**
$\nu_{O\text{-}H}$	3415	3442	3383	3442
$\nu_{C\text{-}H}$	2977, 2883	2925, 2854	2922, 2872	2922, 2854
$\nu_{as\,(COO^-)}$	1679	1570	1637	1610
$\nu_{s\,(COO^-)}$	1427	1386	1379	1384
$\nu_{C=C}/\nu_{C=N}$	1602, 1577, 1471	1490	1521, 1492	1521, 1488
$\nu_{C\text{-}N}$	1120	1120	1124	1120
$\delta_{(Ar\text{-}H)}$	858, 767	852, 777	858, 779	858, 792

Table S5. Detailed attribution of the UV-vis spectra of H_2MCTCA and complexes **1-3.**

Complexes	Wavelength (nm)	Transition	Types
H_2MCTCA	275	π-π*	LLCT
	370	n-π*	LLCT
1	270	π-π*	LLCT
	500	N-Pb	LMCT
2	272	π-π*	LLCT
	344	n-π*	LLCT
	500	N-Co	LMCT
3	272	π-π*	LLCT
	345	n-π*	LLCT
	496	N-Cu	LMCT

Table S6. Fluorescence sensing results of complex **1** for Azi., Col. and Bal..

	Concentration (mol/L)	K_{SV} (M^{-1})	R^2	*LOD* (μM)	Fluorescence quenching rate (%)
Azi.	10^{-4}	7.11×10^4	0.9969	0.28	53.62
Col.	10^{-4}	6.66×10^4	0.9941	0.30	56.85
Bal.	10^{-4}	1.55×10^5	0.9972	0.13	66.75

Table S7. Fluorescence sensing results of complex **1** for Th^{4+} and UO_2^{2+}.

	Concentration (mol/L)	K_{SV} (M^{-1})	R^2	*LOD* (μM)	Fluorescence quenching rate (%)
Th^{4+}	10^{-3}	7.55×10^3	0.9950	2.63	60.36
UO_2^{2+}	10^{-3}	7.79×10^3	0.9934	2.55	49.37

Table S8. The lifetimes fitting parameters of complex **1** before and after detection.

	Lifetime (ns)	Average lifetime (ns)	CHISQ*
1	$\tau_1 = 8.92$ $\tau_2 = 36.8$ $\tau_3 = 2.31$	3.10	1.38
1+Azi.	$\tau_1 = 8.11$ $\tau_2 = 54.9$ $\tau_3 = 1.67$	2.14	1.73
1+Col.	$\tau_1 = 8.63$ $\tau_2 = 31.3$ $\tau_3 = 1.80$	2.76	1.48
1+Bal.	$\tau_1 = 3.62$ $\tau_2 = 1.70$ $\tau_3 = 15.8$	1.84	1.72
1+ Th^{4+}	$\tau_1 = 8.63$ $\tau_2 = 54.7$ $\tau_3 = 1.63$	2.00	1.71
1+ UO_2^{2+}	$\tau_1 = 1.036$ $\tau_2 = 1.31$ $\tau_3 = 12.2$	1.26	1.59

*CHISQ is the discrepancy between fitted equations and data

References

[1] Sheldrick G M. A short history of SHELX. Acta Crystallographica Section A: Foundations and Advances, 2008, 64: 112-122.

[2] Dolomanov O V, Bourhis L J, Gildea R J, et al. OLEX2: a complete structure solution, refinement and analysis program. Journal of Applied Crystallography, 2009, 42: 339-341.

[3] Spek A L. Single-crystal structure validation with the program PLATON. Journal of Applied Crystallography, 2003, 36: 7-13.